

Transport Barriers Formation and Properties Study Based on Bifurcation Concept

T. Onjun¹, B. Chatthong¹, R. Picha², N. Poolyarat³ and J. Promping²

¹*School of Manufacturing Systems and Mechanical Engineering, Sirindhorn International Institute of Technology, Thammasat University, Pathum Thani, Thailand*

²*Thailand Institute of Nuclear Technology, Bangkok, Thailand*

³*Department of Physics, Thammasat University, Pathum Thani, Thailand*

A coupled 2-fields bifurcation model is used to study the formations of both edge transport barrier (ETB) and internal transport barrier (ITB) in tokamak plasmas. In this work, the heat and particle transport equations can be written, respectively, in slab geometry as:

$$\frac{3}{2} \frac{\partial p}{\partial t} - \frac{\partial}{\partial x} [\chi_{neo} + \chi_{ano} f_s(v'_E, s)] \frac{\partial p}{\partial x} = H(x) \text{ and } \frac{\partial n}{\partial t} - \frac{\partial}{\partial x} [D_{neo} + D_{ano} f_s(v'_E, s)] \frac{\partial n}{\partial x} = S(x), \text{ where}$$

p is the plasma pressure, n is the plasma density, χ_{neo} and D_{neo} are the heat and particle neoclassical transport coefficients, respectively, χ_{ano} and D_{ano} are the heat and particle anomalous transport coefficients, respectively, f_s is a suppression function which is assumed to depend on the flow shear v'_E and the magnetic shear s , and $H(x)$ and $S(x)$ are the thermal and particle sources, localized at plasma center and edge, respectively. Furthermore, it is assumed that only the anomalous channel is suppressed by the two mechanisms with the suppression

$$\text{function of the form: } f_s(v'_E, s) = \frac{\beta |s|}{1 + \alpha v'^2_E} \frac{1}{1 + \gamma s^2}, \text{ where } \alpha, \beta, \text{ and } \gamma \text{ are arbitrarily chosen}$$

constants representing strengths of the suppression. This function is based on assumptions that the transports can be quenched or reduced by the flow shear and magnetic shear. Furthermore, the flow shear strength is also affected by the magnetic shear that is the magnetic topology also influences the flow in the plasma. The flow shear couples the two

$$\text{transport equations according to the force balance equation: } v'_E = c \frac{E'_r}{B} \square - \frac{c}{eBn^2} p'n', \text{ where } E_r$$

is the radial electric field and B is plasma magnetic field. Note that for simplicity, the effects of curvature, toroidal rotation, and poloidal rotation are neglected. The magnetic shear s is calculated

$$\text{from the } q\text{-profile as follows: } s = \frac{x}{q} \frac{\partial q}{\partial x}, \quad q = \frac{x}{R} \frac{B_\phi}{B_\theta}, \text{ where } B_\phi \text{ and } B_\theta \text{ are toroidal and poloidal}$$

magnetic fields, respectively. A large aspect ratio tokamak of circular cross section approximation is assumed throughout the work. The toroidal magnetic field is assumed to be constant; while the

poloidal magnetic field is calculated from the current using Ampere's law with current density of the form: $j(x) = j_0 \left(1 - (x - x_0)^2/a^2\right)^{\nu} + j_b$, where x_0 is the location of current density peak, a is the plasma minor radius and j_b is the bootstrap current which is locally proportional to pressure gradient ($j_b \propto -\nabla p$) [1]. Both transport equations can be decoupled using the method similar to that in Ref. [2]. Then, using the given current density and sources profiles the plasma pressure/density and their respective gradients can be numerically solved. All numerical results obtained are carried out using the same set of chosen constants; otherwise it is specified promptly. The transport coefficients are defined such that both thermal and particle anomalous diffusivities are around one order of magnitude over their neoclassical counterparts. The assumption is valid for ions, while for electrons the order of magnitude can be as high as two. In addition, the particle diffusivities are set to be roughly a quarter of thermal diffusivities [3]. Specifically, $\chi_{neo} = 1$, $\chi_{ano} = 10$, $D_{neo} = 0.25$, $D_{ano} = 2.5$, $\alpha = 0.1$, $\beta = 1$, and $\gamma = 0.1$. These values of transport coefficients are in a typical range of transport predicted by simulations using integrated predictive modeling codes using predictive core transport models [4-5].

Plasma Profiles and Bifurcation Diagram

Four scenarios are considered in this work. Scenarios 1 and 3 are the scenarios with the same heating which is less than the critical value required for *L-H* transition ($Q_L = 0.92Q_{L \rightarrow H}$), but with different location of current density peaking; at $x_0 = 0$ (plasma center), $x_0 = 0.2$ and $x_0 = 0.1$, respectively. On the other hand, scenarios 2 and 4 are the scenarios with the same heating which is more than the critical value required for *L-H* transition ($Q_H = 1.06Q_{L \rightarrow H}$), but with different location of current density peaking at; $x_0=0$ (plasma center), $x_0 = 0.2$ and $x_0 = 0.1$, respectively. It can be seen that each scenario yields the plasma with different performance. Firstly, there exists a heating threshold $Q_{L \rightarrow H}$ in which the plasma makes a transition from *L*-mode to *H*-mode with formation of an edge transport barrier (ETB) near plasma edge. In scenario 1, the plasma is set up with low heat source and no reverse shear profile (current profile peak at plasma center). This plasma remains in *L*-mode with central pressure and density equal to 0.69 and 0.77, respectively. Scenario 2 is setup with heat source greater than the critical value required for *L-H* transition ($Q_H > Q_{L \rightarrow H}$) and no reverse shear profile. In this scenario, the plasma makes a transition to *H*-mode with a pedestal width of 0.038 and central pressure and density of 1.24 and 1.42, respectively. Numerically, the heating in scenario 2 increases from that of scenario 1 by 15% but the central plasma pressure and density are almost doubled. This is a very significant enhancement which is why the *H*-

mode is preferred for tokamak operation. The bottom panels illustrate bifurcation diagram which mapped numerical results of each scenario into heat flux Q versus pressure gradient p' and particle flux Γ versus density gradient n' spaces. Theoretically, an example of a tradition *s*-curve bifurcation diagram can be found in Ref. [2] which shows a non-monotonic behavior. In figure 1, there appear discontinuities in pressure and density gradient profiles for scenario 2. They identify the locations of top of ETB.

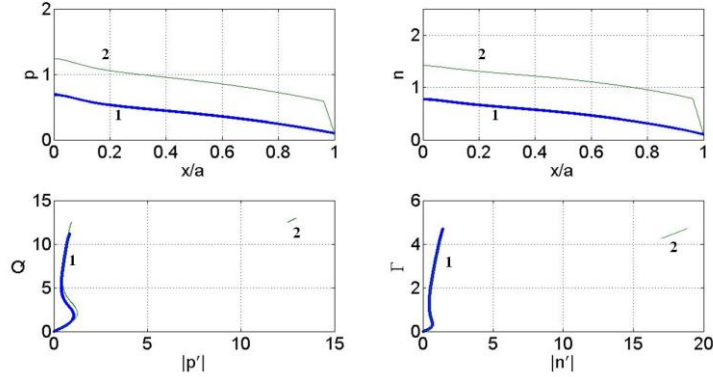


Figure 1: Pedestal Plasma pressure (top left) and density (top right) as a function of normalized minor radius x/a for setup scenarios 1 (thick line) and 2 (thin line), and the results mapped onto heat flux versus pressure gradient (bottom left) and particle flux versus density gradient (bottom right).

Scenario 3 is the scenario with low heat source ($Q_L < Q_{L \rightarrow H}$) and current profile peaking at $x/a = 0.2$ ($x_0 = 0.2$) representing reversed shear profile. In this case, the plasma is still in *L*-mode but there is a formation of ITB near plasma core (see figure 2). The central pressure and density are around 1.23 and 1.36, which are increased from *L*-mode plasma without ITB by 78% and 77%, respectively. This implies that appropriate control of current profile in the plasma can lead to enhancement of plasma performance as well. The simulations in this work assume a form of current density distribution [3] with possibility to change the current peak location and with addition of bootstrap current effect. Scenario 4 is setup with high heat source ($Q_H > Q_{L \rightarrow H}$) and current profile peaking at $x/a = 0.2$. As expected based on the previous results, ETB and ITB formations can occur simultaneously. Note that the top of ITB appears to be closed to the location of current drive peak. The central pressure and density are increased to 1.94 and 2.06 which are 181% and 168% enhancement over *L*-mode performance, respectively. In this particular scenario, the jump in the gradients at lowest value of Q corresponds to the top of ITB, next jump corresponds to the foot of ITB and the jump at highest value of Q corresponds to the top of ETB.

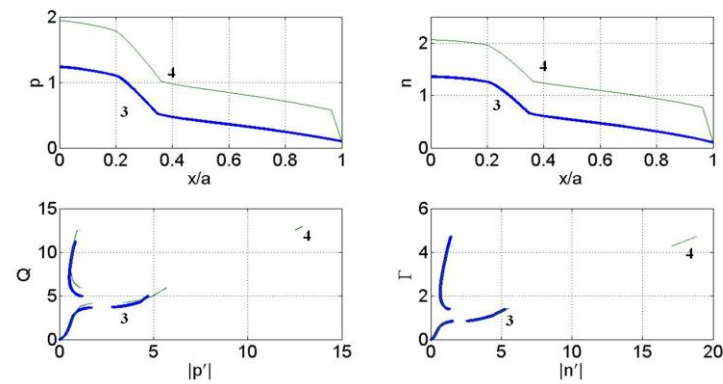


Figure 2: Plasma pressure (top left) and density (top right) as a function of normalized minor radius x/a for setup scenarios 3 (thick line) and 4 (thin line), and the results mapped onto heat flux versus pressure gradient (bottom left) and particle flux versus density gradient (bottom right).

Conclusions

A coupled 2-fields bifurcation model is considered to analyze the formation and properties of ETB and ITB in tokamak plasmas. The transport equations for temperature and particle are self-consistently solved for the relation between local plasma gradients and corresponding fluxes in order to examine the ETB and ITB formations. It is found that the bifurcation nature can be observed when mapped onto fluxes versus gradients space in which abrupt changes in the gradients can be observed at plasma edge for ETB and plasma core for ITB. ETB formation depends sensitively on the heat flux. On the other hand, ITB formation is possible only with a presence of reverse magnetic shear profile with its width depends weakly on the heat flux.

Acknowledgments

This work was supported by the Commission on Higher Education (CHE) and the Thailand Research Fund (TRF) under Contract No.RSA5580041. B Chatthong thanks the Royal Thai Scholarship, Bangchak Petroleum PCL, and Thailand Institute of Nuclear Technology for financial support.

References

- [1] R J Bickerton, J W Connor, and J.B. Taylor *Nature physical science*, **229** 110-112 (1971)
- [2] M. A. Malkov, and P. H. Diamond *Phys. Plasmas*, **15** 12, 122301 (2008)
- [3] John Wesson, Tokamaks, New York, USA: Clarendon Press 2004
- [4] David Hannum, Glenn Bateman, Jon Kinsey *et al. Phys. Plasmas*, **8** 3, 964-974 (2001)
- [5] Thawatchai Onjun, Glenn Bateman, Arnold H. Kritz *et al. Phys. Plasmas*, **8** 3, 975-985 (2001)